frontiers | Frontiers in Aging Neuroscience

TYPE Original Research
PUBLISHED 29 April 2025
DOI 10.3389/fnagi.2025.1549770

OPEN ACCESS

EDITED BY
Daniel Ortuño-Sahagún,
University of Guadalajara, Mexico

REVIEWED BY
Karsten Baumgaertel,
AMPLIO Consultants LLC, United States
Adriana Ximenes-da-Silva,
Federal University of Alagoas, Brazil
Karina Hernández Ortega,
National Autonomous University of Mexico, Mexico
Mary B. Kennedy,
California Institute of Technology, United States

*CORRESPONDENCE
Amy F. T. Arnsten
✉ amy.arnsten@yale.edu
Angus C. Nairn
✉ angus.nairn@yale.edu

†These authors have contributed equally to this work

RECEIVED 21 December 2024
ACCEPTED 07 April 2025
PUBLISHED 29 April 2025

CITATION
Bathla S, Datta D, Bolat D, Woo E, Duque A, Arellano JI, Arnsten AFT and Nairn AC (2025) Dysregulated calcium signaling in the aged macaque entorhinal cortex associated with tau hyperphosphorylation.
Front. Aging Neurosci. 17:1549770.
doi: 10.3389/fnagi.2025.1549770

Dysregulated calcium signaling in the aged macaque entorhinal cortex associated with tau hyperphosphorylation

Shveta Bathla[1†], Dibyadeep Datta[1†], Dinara Bolat[2], Elizabeth Woo[2], Alvaro Duque[2], Jon I. Arellano[2], Amy F. T. Arnsten[2*] and Angus C. Nairn[1*]

[1]Department of Psychiatry, Yale University School of Medicine, New Haven, CT, United States, [2]Department of Neuroscience, Yale University School of Medicine, New Haven, CT, United States

Introduction: Tau pathology in sporadic Alzheimer's disease (AD) follows a distinct pattern, beginning in the entorhinal cortex (ERC) and spreading to interconnected brain regions. Early-stage tau pathology, characterized by soluble phosphorylated tau, is difficult to study in human brains post-mortem due to rapid dephosphorylation.

Methods: Rhesus macaques, which naturally develop age-related tau pathology resembling human AD, provide an ideal model for investigating early tau etiology. This study examines the molecular processes underlying tau pathology in the macaque ERC, focusing on calcium and inflammatory signaling pathways using biochemical and immunohistochemistry.

Results: Our findings reveal an age-related decrease in PDE4 phosphodiesterase that hydrolyzes cAMP and increases in calpain-2 and glutamate carboxypeptidase II that occur in parallel with early-stage tau hyperphosphorylation at multiple epitopes (pS214-tau, pT181-tau, pT217-tau).

Discussion: These findings suggest that dysregulated calcium signaling in ERC, beginning in middle-age, may prime tau for hyperphosphorylation, potentially driving the early stages of AD, advancing our understanding of how ERC vulnerabilities contribute to neurodegeneration in AD.

KEYWORDS

entorhinal cortex, tau pathology, cAMP-calcium signaling, Alzheimer's disease, calpain-2, GCPII, PDE4 phosphodiesterase, inflammation

Introduction

Tau pathology in sporadic Alzheimer's disease (AD) exhibits a stereotypical progression pattern with neurofibrillary tangles (NFTs) in cortex forming earliest in the rhinal cortices, especially in the entorhinal (ERC) and transentorhinal cortex (Braak and Braak, 1991; Braak and Braak, 1992; Braak and Del Trecidi, 2015; Braak and Del Tredici, 2015; Hyman et al., 1986; Kaufman et al., 2018). Notably, NFTs appear in middle age, distinctly in layer II cell islands in the ERC (Braak and Del Tredici, 2015; Liu and Li, 2019), where they impair axonal transport and consequently lead to loss of neuronal function. Evidence from studies in humans and animal models indicates that tau pathology spreads from the ERC to interconnected glutamatergic neurons in the limbic and association cortices,

as well as hippocampus, seeding pathology throughout higher brain circuits, with primary sensory cortices impacted only at end stage disease (Ahmed et al., 2014; Calafate et al., 2015; Colin et al., 2020; de Calignon et al., 2012; Dujardin et al., 2018; Fu et al., 2018; Kaufman et al., 2018; Lewis et al., 1987). The accumulation of abnormal tau in the ERC is one of the first events in AD and precedes memory deficits and cognitive decline (Zhang et al., 2024). Therefore, illuminating why the ERC is highly susceptible to tau pathology is critical to uncovering the etiology of the common, late-onset, sporadic form of AD. However, the earliest stage, soluble phosphorylated tau is difficult to study in human brains except by using biopsy samples, as it can be rapidly dephosphorylated post-mortem within a few hours after death (Matsuo et al., 1994; Wang et al., 2015). Thus, preclinical animal models are needed to study the early etiology of tau pathology.

Rhesus macaques (Macaca mulatta) naturally develop tau pathology with advancing age, with the same *qualitative* features as human patients with AD, and thus can be utilized to understand why ERC circuits are especially vulnerable (Paspalas et al., 2018). Age-related decline in cognitive performance and reduced novelty preference in the visual paired comparison (VPC) task was observed in aged macaques (Herndon et al., 1997; Insel et al., 2008). Importantly, AT8-labeled (pS202/pT205-tau) NFTs can be seen in macaques of extreme age, with paired helical filaments identical to human (Paspalas et al., 2018). The pattern and sequence of cortical tau pathology in macaques is also the same as in humans, first arising in the ERC layer II cell islands, and then extending into deeper ERC layers, the hippocampus, limbic and association cortices, with little expression in primary visual cortex (Arnsten et al., 2021a; Arnsten et al., 2019; Arnsten et al., 2021b; Paspalas et al., 2018). Importantly, extremely short post-mortem intervals are possible when analyzing rhesus macaque brains, which allows the analysis of early, soluble forms of hyperphosphorylated tau. This includes the capture of tau phosphorylated at threonine 181 (pT181-tau) and threonine 217 (pT217-tau), tau species used as fluid-based biomarkers in humans, where pT217-tau in particular is being developed as a plasma biomarker for incipient AD (Barthelemy et al., 2020; Hansson et al., 2023; Janelidze et al., 2020; Mattsson-Carlgren et al., 2023; Olsson et al., 2016; Salvado et al., 2023).

Longstanding research has suggested that calcium dysregulation might be a crucial precipitating factor in AD pathogenesis (Alzheimer's Association Calcium Hypothesis, 2017; Gibson and Peterson, 1987; Khachaturian, 1994). Research from aging macaques has corroborated this hypothesis, showing that excitatory cells in vulnerable association cortices such as the ERC and the dorsolateral prefrontal cortex (dlPFC) express the molecular machinery for cAMP-protein kinase A (PKA) actions to magnify calcium signaling, particularly within dendrites and dendritic spines, and that dysregulation with age and/or inflammation contributes to tau hyperphosphorylation (Arnsten et al., 2020; Arnsten et al., 2021c; Arnsten and Wang, 2020). For example, cAMP-calcium regulation by PDE4D and mGluR3 are reduced in the aged macaque dlPFC (Arnsten et al., 2021b; Datta et al., 2020). Elevated PKA signaling phosphorylates ryanodine receptors (pRyR2) on the SER to cause calcium leak into the cytosol, which is seen in the aged dlPFC and in middle age in the more vulnerable ERC (Datta et al., 2021; Paspalas et al., 2018), and has been documented in the brains of patients with AD (Lacampagne et al., 2017). Very high levels of cytosolic calcium can activate calpain-2, which cleaves and activates GSK3β and p25-cdk5 contributing to the hyperphosphorylation of tau (Arnsten et al., 2021b; Arnsten et al., 2021c; Baudry et al., 2013). In addition, glutamate carboxypeptidase II (GCPII) inflammatory signaling destroys N-acetyl-aspartyl-glutamate (NAAG), the native ligand for mGluR3 (Yang et al., 2022), and GCPII activity correlates with pT217-tau levels in the aged dlPFC (Bathla et al., 2023), emphasizing the importance of this mechanism to understanding tau pathology.

However, it is not known if signs of dysregulated calcium signaling can be seen in association with hyperphosphorylated tau in the macaque ERC, where cortical tau pathology first begins. These relationships were explored in the current study of rhesus macaque ERC, utilizing both biochemistry and immunohistochemistry to examine molecular features of pathology with advancing age. We examined the expression patterns of early stage, soluble phosphorylated tau (pS214-tau, pT181-tau, pT217-tau), as well as the expression of mechanisms that regulate cAMP-calcium signaling (PDE4A, PDE4D, mGluR3), and those that drive pathology (S2808RyR2, calpain-2, GCPII) in rhesus macaque ERC across the adult age-span.

Materials and methods

Animals were cared for in accordance with the guidelines of Yale University Institutional Animal Care and Use Committee, and Public Health Service requirements for animal use as described in the Guide for the Care and Use of Laboratory Animals. Yale University is accredited by the American Association for Accreditation of Laboratory Animal Care (AAALAC).

Animal and tissue processing for biochemistry

Rhesus monkeys used for biochemical experiments ranged in age from 8.3 to 28.6 years (N = 10, all female). Animals were divided between young (< 18 years) and aged (> 18 years) using an age cut-off that we and other researchers have utilized (Bartus et al., 1978). Post-mortem interval (PMI) was kept as short as possible (8–30 min) as longer PMI is likely to have an impact on tissue quality and more specifically on levels of phosphorylation. For tissue collection, the dura was removed, and ERC tissue taken out using a scalpel. Immediately following dissection samples were placed into liquid nitrogen and stored at −80°C for further use. For comparative purpose, we have included samples from a 19.5 years-old monkey, previously found to have unusually low levels of phosphorylated tau (Datta et al., 2021; Leslie et al., 2021), but have not included it in the data analysis.

Protein extraction

Brain tissue (ERC, 100 mg) was lysed in 1% Triton X-100 lysis buffer (200 mM NaCl, 10 mM HEPES, 10 mM EGTA, 10 mM EDTA, phosSTOP phosphatase inhibitor, and cOmplete mini protease inhibitor) with 20 strokes by hand in a glass-teflon homogenizer. Cell debris was removed by centrifugation for 15 min

(13,000 × *g*) at 4°C. The supernatant was collected, and protein concentration was determined with Bradford Assay (Bio-Rad, USA). The supernatant was stored at −80°C for further use.

Immuno-blotting

Protein (40 μg per lane) was boiled for 5 min at 100°C in SDS-loading buffer with DTT. The samples were separated on 4%–20% Tris-glycine gels using 150 V over 1.5 h in a Criterion cell (Bio-Rad, United States). Proteins were transferred onto 0.45 μm nitrocellulose membranes at 300 mA for 1.5 h in a Criterion blotter (Bio-Rad, United States). After 1 h blocking at room temperature in TBST (20 mM Tris-HCl, 140 mM NaCl, pH 7.5, 0.05% Tween-20) containing 3% bovine serum albumin (BSA), membranes were probed overnight with antibodies:pS214-tau (Abcam ab4846, 1:1000, RRID:AB_304678), pT181-tau (CST12885S,1:1000, RRID:AB_2798053), pT217-tau antibody (AS-54968; AnaSpec, 1:1000, RRID:AB_2173656), calpain-2 (Abcam ab39165,1:1000, RRID:AB_725844), PDE4A (Abcam ab14607,1:1000, RRID:AB_301375), PDE4D (Millipore ABS22, 1:1000, RRID:AB_10807152), mGluR3 (Abcam AB166608,1:1000, RRID:AB_2833092), phospho-RyR S2808 (Abcam ab59225 1:500, RRID:AB_946327), GAPDH (Millipore CB1001-500, 1:10,000, RRID:AB_2107426), GCPII (Proteintech, 13163-1-AP,1:1000, RRID:AB_2106442) in TBST containing 3% BSA at 4°C. Membranes were washed three times with TBST and incubated with fluorescent secondary antibodies (1:10000) of the appropriate species for 1 h at room temperature. Three TBST washes were used to remove secondary antibody. Blots were rinsed with Milli-Q water and analyzed using a LI-COR Odyssey scanner.

Statistical analysis of biochemical data

Image Studio Lite was used for band quantification and background subtraction. Prior to quantification, background subtraction was done by calculating the average intensity immediately above and below the band(s) of interest. The expression of targets was further normalized by calculating the ratio of band intensity of target/band intensity GAPDH. For statistical comparison, unpaired *t*-test with Welch's correction was performed on the grouped analysis as markers were normally distributed. The normalized data was plotted using Graphpad Prism software. The correlation analysis between age and targets (phosphorylated tau and calcium regulatory proteins) was determined by Pearson correlation.

Immunohistochemistry

Animals and tissue preparation

Four aged (24, 28, 30, and 31 years) female rhesus macaques (*Macaca mulatta*) were used for this study. As described previously (Datta et al., 2020; Datta et al., 2021; Jin et al., 2018b; Paspalas et al., 2013), rhesus macaques were deeply anesthetized prior to transcardial perfusion of 100 mM phosphate-buffer saline (PBS), followed by 4% paraformaldehyde/0.05% glutaraldehyde in 100 mM PBS. Following perfusion, a craniotomy was performed, and the entire brain was removed and dissected, including a frontal block containing the primary region of interest. The brains were sectioned coronally at 30 μm on a vibratome (Leica) across the entire rostrocaudal extent of the entorhinal cortex (ERC). The free-floating sections were cryoprotected in a solution containing ethylene glycol (30%), glycerol (30%) in 200 mM phosphate buffer (PB) and stored at −20°C. The number of subjects was necessarily small, given the scarcity of macaques since their extensive use to develop SARS-cov-2 vaccines.

Histology and immunoreagents

We used previously well-characterized primary antibodies raised in rabbit and mice. We used an affinity isolated polyclonal PDE4D protein (SAB4502128; Millipore Sigma Aldrich, Burlington, MA; RRID:AB_10744568) raised against amino acids 156-205 of PDE4D that recognizes human and rodent PDE4D based on sequence homology. The antibody is highly specific and detects endogenous levels of total PDE4D protein at a band migrating at ~91 kDa. The antibody is suited for a range of applications, including immunohistochemistry, immune-blotting and ELISA as per manufacturer's recommendations. The specificity and selectivity of the PDE4D antibody has been previously characterized using immunohistochemistry in myocytes to identify a role of PDE4D-PRKAR1α in cardiac contractility (Bedada et al., 2016) and with immunohistochemistry and immunoEM in rhesus macaque dlPFC (Datta et al., 2020). We used a rabbit anti-pT217-tau at 1:200 (cat# AS-54968, Anaspec, RRID:AB_2173656). The immunogen used KLH conjugated with a synthetic phosphopeptide corresponding to human tau at phosphorylated threonine 217. We used a mouse anti-phosphoSer214-tau IgM (clone CP3) at 1:200 (generously provided by Dr. Peter Davies, The Feinstein Institutes for Medical Research) and a mouse anti-phosphoThr181-tau IgG1k (clone AT270) at 1:200 (MN1050; Thermo Fisher Scientific, RRID:AB_223651), antibodies that have been extensively validated by our group using immunohistochemistry and immunoelectron microscopy in rhesus macaque association cortices (Datta et al., 2021; Paspalas et al., 2018). For calpain-2, we used a rabbit anti-calpain-2 IgG at 1:200 (ab39165; Abcam, RRID:AB_725844). The immunogen is a synthetic peptide based on the amino terminal end of domain-III in the large subunit of calpain-2 that does not cross-react with other calpain family members and has been extensively validated in several protocols including immunohistochemistry, immunocytochemistry and immunofluorescence approaches as per the manufacturer.

Single-label immunoperoxidase immunohistochemistry

For single-label immunoperoxidase immunohistochemistry, sections of ERC were transferred for 1 h to Tris-buffered saline (TBS) containing 5% BSA, plus 0.05% Triton X-100 to block non-specific reactivity, and incubated in primary antibodies in TBS for 72 h at 4°C. The tissue sections were incubated in goat anti-rabbit and goat anti-mouse biotinylated antibodies (Vector Laboratories) at 1:300 in TBS for 2 h, and developed using the Elite ABC kit (Vector Laboratories) and diaminobenzidine (DAB) as a chromogen. Omission of the primary antibody eliminated all labeling. Sections were mounted on microscope slides and ERC cortical layers were photographed under an Olympus BX51 microscope equipped with a Zeiss AxioCam CCD camera. Zeiss AxioVision imaging software was used for imaging and data acquisition.

Results

Age-related increases in tau phosphorylation in rhesus macaque ERC

Biochemical analyses can accurately measure levels of soluble, phosphorylated tau. The current study assayed tau phosphorylated at S214, T217, and T181, three key early sites propelling tau pathology. We first quantified pS214-tau and observed significantly higher pS214-tau expression levels in aged monkeys compared to young (Figures 1A, B, $^{***}P$ = 0.0009) in ERC. We found a trend-level positive correlation (P = 0.0517) between the expression of pS214-tau and age in rhesus macaque ERC (Figure 1C). We further analyzed two additional phosphorylation sites (pT181-tau and pT217-tau) that have emerged as highly sensitive fluid-based biomarkers for the early identification of patients at risk of developing AD. pT181-tau expression was higher in aged macaques than in younger animals (Figures 2A, B, $^{**}P$ = 0.0028) in ERC. Furthermore, the level of pT181-tau showed a trend-level positive correlation (Figure 2C, P = 0.218) with advanced age. Aged macaques also had significantly higher expression of pT217-tau (Figures 3A, B, $^{*}P$ = 0.0255) compared to young animals in ERC, with a trend-level positive correlation between pT217-tau and age-span in rhesus macaque ERC (Figure 3C, P = 0.3287). Similar to previous studies in dlPFC (Datta et al., 2021; Leslie et al., 2021), the levels of S214, T181 and T217 were low in ERC from the 19.5 year-old monkey.

We used immunohistochemistry to localize pS214-tau, pT181-tau, and pT217-tau in aged macaque ERC (ages 24–31 years). We found robust immunolabeling for pS214-tau (Figures 1D–F), pT181-tau (Figures 2D–F), and pT217-tau (Figures 3D–F) phosphorylation epitopes in ERC across the cortical neuropil, including prominent labeling in stellate cells in layer II, and pyramidal cells in layer III and layers V–VI. Immunolabeling was evident in perisomatic compartments and along apical dendrites, in excitatory neurons.

Age-related calcium dysregulation in ERC

Previous research indicated that calcium dysregulation occurs very early in the ERC (Paspalas et al., 2018), which may help to explain why this area is the first to show cortical tau pathology. Thus, the current study examined whether there would be signs of excessive cytosolic calcium in the aged ERC, as well as evidence of reduced mGluR3 and PDE4 regulation of cAMP drive on calcium signaling.

pS2808-RyR2 expression in aged rhesus macaque ERC

PKA phosphorylation of RyR2 causes calcium leak from the SER into the cytosol, and has already been documented in the ERC of young adult macaques aged 7–9 years (Paspalas et al., 2018). Consistent with previous research, there was already extensive expression of pS2808-RyR2 in macaques in this age range, with no further increase with advancing age (Figures 4A, B, P = 0.9307), and no correlation between age and pS2808-RyR2 levels (Figure 4C, P = 0.8808).

Calpain-2 expression in aged rhesus macaque ERC

In contrast to calpain-1, which is activated by normal physiological levels of calcium, calpain-2 is activated by very high levels of cytosolic calcium (Baudry et al., 2013; Higuchi et al., 2012) and can cleave and activate the kinases that hyperphosphorylate tau (Goñi-Oliver et al., 2007). The expression of calpain-2 was significantly higher in aged macaque ERC than in young animals (Figures 5A, B, $^{**}P$ = 0.0052), and there was a trend for a positive correlation with calpain-2 levels and age in rhesus macaque ERC (Figure 5C, P = 0.1473). In aged macaque ERC, using brightfield microscopy we observed calpain-2 immunolabeling in layer II stellate cell islands (Figure 5D), as well as in pyramidal cells in layer III (Figure 5E), and layer V–VI (Figure 5F), often expressed within apical dendrites with a twisted morphology, e.g., calpain-2 immunolabeling in layer V–VI (Figure 5F), common in neurofibrillary tangles (Figures 5D–F).

Phosphodiesterase expression in aged rhesus macaque ERC

In young adult macaques, phosphodiesterases PDE4A and PDE4D are localized on the SER, positioned to regulate cAMP-PKA, with PDE4A generally limited to dendritic spines, and PDE4D more widely expressed with significant expression in dendrites (Carlyle et al., 2014; Datta et al., 2020; Datta et al., 2021). We found that PDE4D expression in macaque ERC decreased significantly with age (Figures 6A, B, $^{*}P$ = 0.0252), while there was a modest non-significant reduction in PDE4A (Figures 6D, E, P = 0.7252) expression in macaque ERC. Furthermore, there was a highly significant negative correlation between PDE4D expression and age (Figure 6C, $^{**}P$ = 0.0070). In contrast, expression of PDE4A was not correlated with age (Figure 6F, P = 0.5048).

mGluR3 and GCPII expression in aged rhesus macaque ERC

Post-synaptic mGluR3 in ERC are positioned to regulate cAMP drive on internal calcium release, a process that is reduced under inflammatory conditions by GCPII catabolism of N-acetylaspartylglutamate (NAAG), the endogenous ligand for mGluR3 (Datta et al., 2023). mGluR3 protein levels in aged macaque ERCs did not show significant changes in the current investigation (Figures 7A, B, P = 0.5205), and levels of mGluR3 were not correlated across age-span (Figure 7C, P = 0.4482). However, GCPII levels did increase with age (Figures 7D, E, $^{*}P$ = 0.0252) and exhibited a trend-level correlation with increasing age-span (Figure 7F, P = 0.3328).

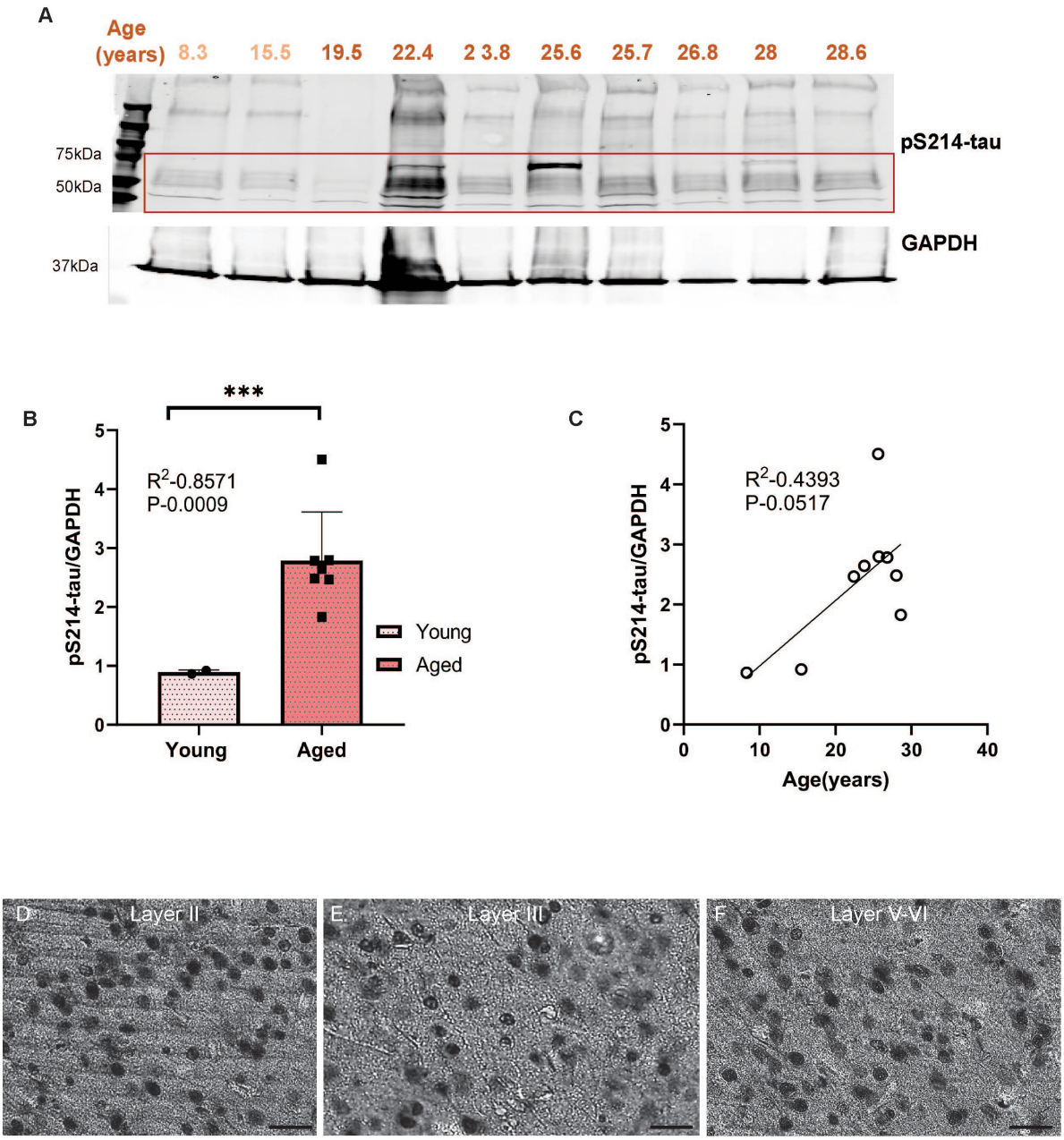

FIGURE 1
(A) Macaque ERC lysate (40 μg) was immunoblotted for pS214-tau (1:1000) and GAPDH (1:10000) across the age span (8.3–28.6 years). Animals are labeled by their age in years and color coded: young animals in light red and aged animals in dark red. **(B)** Expression of pS214-tau normalized by GAPDH is plotted between young (8.3–15.5 years) and aged (22.4–28.6 years). Young animals are denoted by circles and aged animals are denoted by squares. Means between the two groups were compared using a two-tailed unpaired *t*-test (***P = 0.0009). **(C)** The correlation between levels of normalized pS214-tau and age across all animals is fit by a linear regression (R^2 = 0.4393, P = 0.0517). **(D–F)** Immunohistochemistry revealed robust immunolabeling for pS214-tau in aged macaque ERC, particularly in layer II, layer III and layer V–VI, within excitatory neurons along apical dendrites and in the cell body. Scale bar, 50 μm.

Correlations between evidence of dysregulated calcium signaling and tau hyperphosphorylation

We examined potential correlations between measures of cAMP-calcium dysregulation and tau hyperphosphorylation. We found that PDE4D expression had an inverse correlation with pTau levels, where reduced levels of PDE4D moderately correlated with increased levels of pS214-tau (Figure 8A, P = 0.0782), consistent with dysregulated cAMP signaling increasing tau phosphorylation by PKA at S214 (Carlyle et al., 2014; Datta et al., 2021). Reduced levels of PDE4D also correlated with increased levels of pT217-tau (Figure 8B, *P = 0.0352), but showed only a trend level inverse correlation with pT181-tau (P = 0.3643, not shown). Conversely, we found a strong positive correlation between calpain-2 levels and pT181-tau expression (Figure 8C,

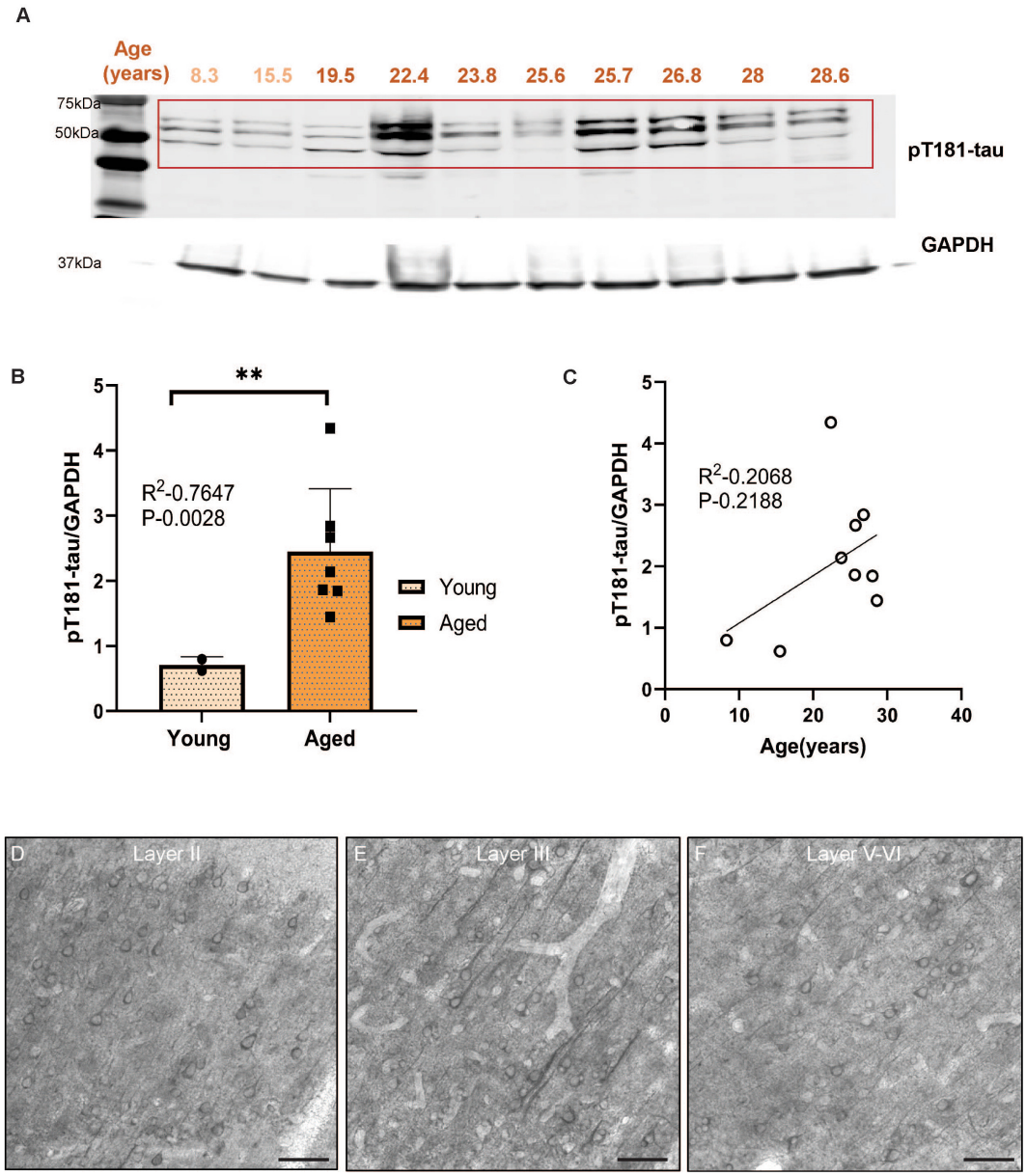

FIGURE 2
(A) Macaque ERC lysate (40 μg) was immunoblotted for pT181-tau (1:1000) and GAPDH (1:10000) across the age span (8.3–28.6 years). Animals are labeled by their age in years and color coded: young animals in light red and aged animals in dark red. **(B)** Expression of pT181-tau normalized by GAPDH is plotted between young (8.3–15.5 years) and aged (22.4–28.6 years). Young animals are denoted by circles and aged animals are denoted by squares. Means between the two groups were compared using a two-tailed unpaired *t*-test (**P = 0.0028). **(C)** The correlation between levels of normalized pT181-tau and age across all animals is fit by a linear regression (R^2 = 0.2068, P = 0.2188). **(D–F)** Immunohistochemistry revealed immunolabeling for pT181-tau in aged macaque ERC, particularly in layer II, layer III and layer V–VI, within excitatory neurons along apical and basilar dendrites and in the cell body. Scale bar, 50 μm.

**P = 0.0095), while the positive correlations between calpain-2 levels and pS214-tau and pT217-tau levels did not reach significance (P = 0.7032 and 0.3951, respectively). There was also a positive correlation between GCPII levels and calpain-2 levels, consistent with reduced mGluR3 regulation of cAMP drive on calcium signaling (Figure 8D, *P = 0.0424). GCPII expression generally correlated with pTau levels, with pT181-Tau levels reaching moderate statistical significance (Figure 8E, P = 0.0511). Correlations with pT217-tau and pS214-tau showed a trend (not shown) but did not reach significance due to a single animal with high levels of tau, but intermediate levels of GCPII, consistent with multiple factors contributing to tau hyperphosphorylation.

Discussion

The current study found increases in phosphorylated tau (pT181-tau, pS214-tau, pT217-tau) and evidence of increased inflammation (GCPII) and calcium dysregulation (calpain-2) in the aged macaque ERC. There was a positive correlation between

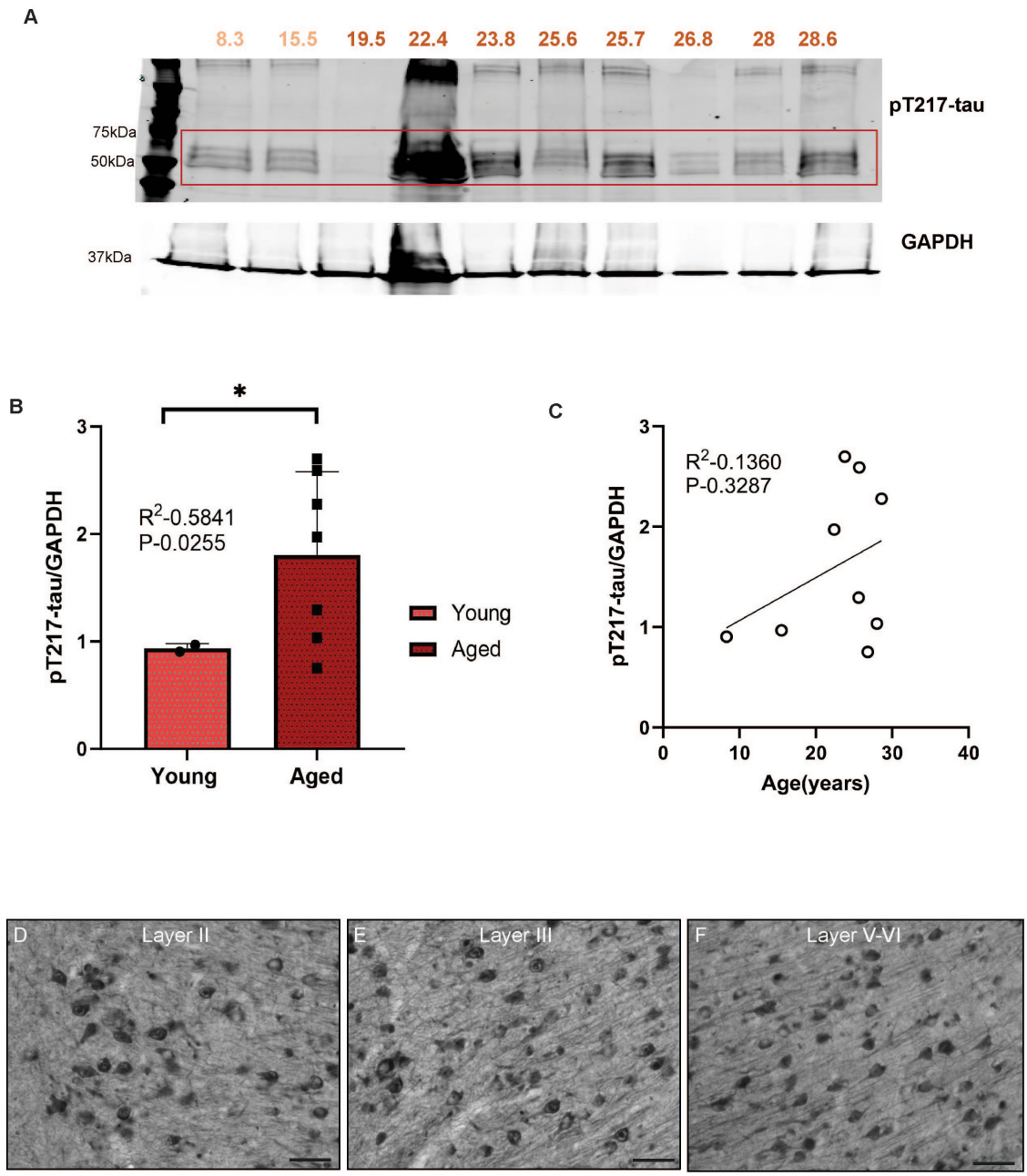

FIGURE 3
(A) Macaque ERC lysate (40 μg) was immunoblotted for pT217-tau (1:1000) and GAPDH (1:10000) across the age span (8.3–28.6 years). Animals are labeled by their age in years and color coded: young animals in light red and aged animals in dark red. **(B)** Expression of pT217-tau normalized by GAPDH is plotted between young (8.3–15.5 years) and aged (22.4–28.6 years). Young animals are denoted by circles and aged animals are denoted by squares. Means between the two groups were compared using a two-tailed unpaired *t*-test (*P = 0.0255). **(C)** The correlation between levels of normalized pT217-tau and age across all animals is fit by a linear regression (R^2 = 0.1360, P = 0.3287). **(D–F)** Immunohistochemistry revealed robust immunolabeling for pT217-tau in aged macaque ERC, particularly in layer II, layer III and layer V-VI, within excitatory neurons along apical and basilar dendrites and in the cell body. Scale bar, 25 μm.

GCPII and calpain-2 levels, consistent with GCPII dysregulating calcium signaling, and general positive correlations between levels of GCPII, calpain and pTau species. Conversely, there were negative correlations between levels of PDE4D and pTau species. These results suggest that age-related loss of PDE4D leads to dysregulation of the cAMP signaling which would exacerbate PKA activity thereby contributing to age-related cognitive decline and neuronal vulnerability (Ramos et al., 2003). The ERC is an essential gateway to the hippocampus for memory formation, and rhesus monkeys begin to develop impaired recognition and relational memory early in the aging process (e.g., 19–23 years, Herndon et al., 1997), consistent with the neurochemical changes seen in the ERC in the current study. Overall, these data indicate an environment of dysregulated cAMP-calcium signaling in the aging ERC that is associated with the rise of early stage, soluble phosphorylated tau. At this early stage, soluble pTau is likely in

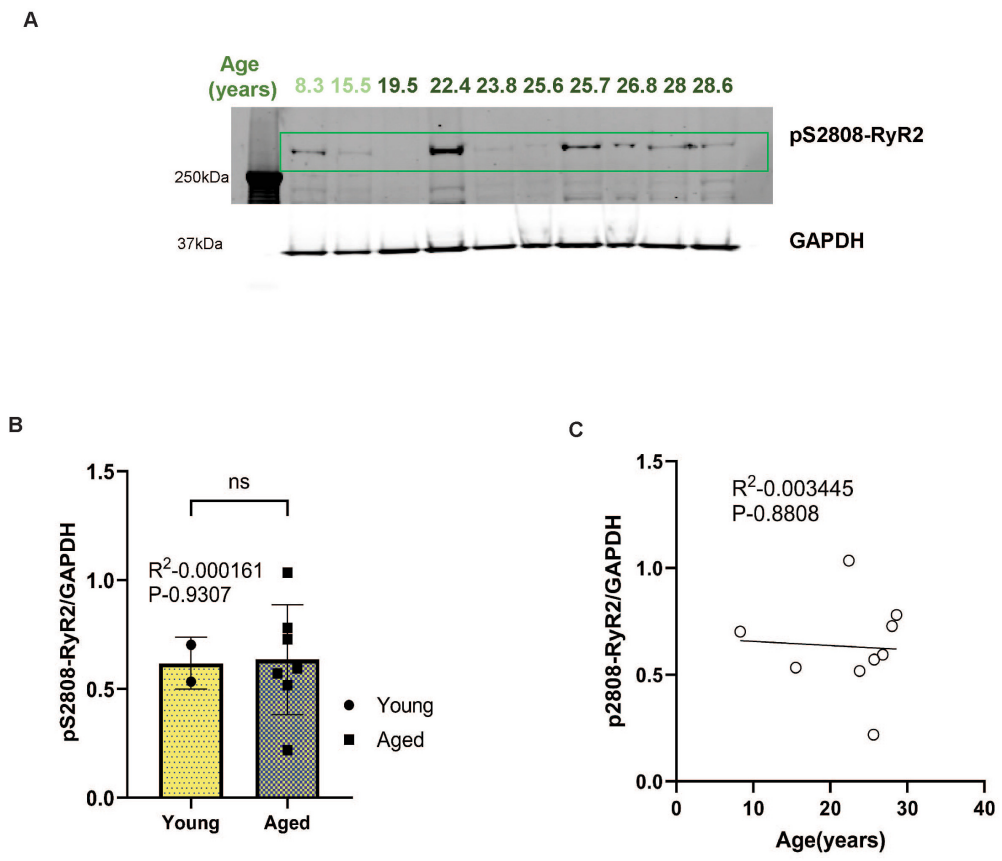

FIGURE 4
(A) Macaque ERC lysate (40 μg) was immunoblotted for pS2808-RyR2 (1:500) and GAPDH (1:10000) across the age span (8.3–28.6 years). Animals are labeled by their age in years and color coded: young animals in light green and aged animals in dark green. **(B)** Expression of pS2808-RyR2 normalized by GAPDH is plotted between young (8.3–15.5 years) and aged (22.4–28.6 years). Young animals are denoted by circles and aged animals are denoted by squares. Means between the two groups were compared using a two-tailed unpaired *t*-test (P = 0.9307). **(C)** The correlation between levels of normalized pS2808-RyR2 and age across all animals is fit by a linear regression (R^2 = 0.0035, P = 0.8808).

the form that traffics between neurons to seed tau pathology in a network of excitatory neurons (Datta et al., 2024), therefore, characterization at this early stage is particularly important for developing informed strategies for disease prevention. The increase in GCPII-regulated inflammation, and its correlations with calpain-2 and pTau levels are of special interest given the likely roles of inflammatory mechanisms in the common, sporadic form of AD, and the previous finding that levels of pT217-tau correlate with GCPII activity in the dlPFC (Bathla et al., 2023). Altogether, these data suggest that targeting inflammation, and specifically calcium dysregulation, may be beneficial in reducing early tau pathology.

Calcium dysregulation plays an important role in tauopathies beyond AD, such as frontotemporal dementia (FTD), progressive supranuclear palsy (PSP), and corticobasal degeneration (CBD) (Katzeff et al., 2020; Webber et al., 2023; Wilson et al., 2023). Research indicates that pathological tau protein accumulation disrupts calcium homeostasis by impairing mitochondrial function, altering endoplasmic reticulum (ER) calcium release, and dysregulating neuronal calcium channels (Kaar et al., 2024). A previous study has shown that iPSCs derived from FTD patients are associated with greater calcium transients, which is associated with an accumulation of pathological tau (Imamura et al., 2016). Furthermore, chemogenetic or pharmacological modulation of calcium influx resulted in an attenuation of misfolded tau accumulation (Whitney et al., 2024). Transcriptomic studies in PSP patients using unbiased snRNA-seq has revealed differential expression of several genes related to calcium signaling modules in neurons, such as calmodulin (CALM1) and calretinin (CALB2). These findings suggest that tau-mediated calcium dysregulation is a common pathological mechanism across tauopathies, driving neuronal vulnerability and disease progression, and highlighting potential therapeutic targets like calcium channel modulators. A weakness of the current study is the relatively small number of subjects, due in large part to the current scarcity of macaques in general given their extensive use in creating SARS-CoV-2 vaccines, and the further rarity of macaques that reach very old age. In particular, larger numbers of subjects may have allowed trends in correlation with age to be significant. It is noteworthy that this type of work is difficult to be done in rodent models that depend on autosomal dominant mutations rather than inflammation to cause pathology, nor in humans, where PMI longer than a few hours limits the opportunity to capture soluble pTau (Matsuo et al., 1994; Wang et al., 2015). Thus, the current data is very valuable for revealing early molecular events in primate ERC related to the rise in tau pathology.

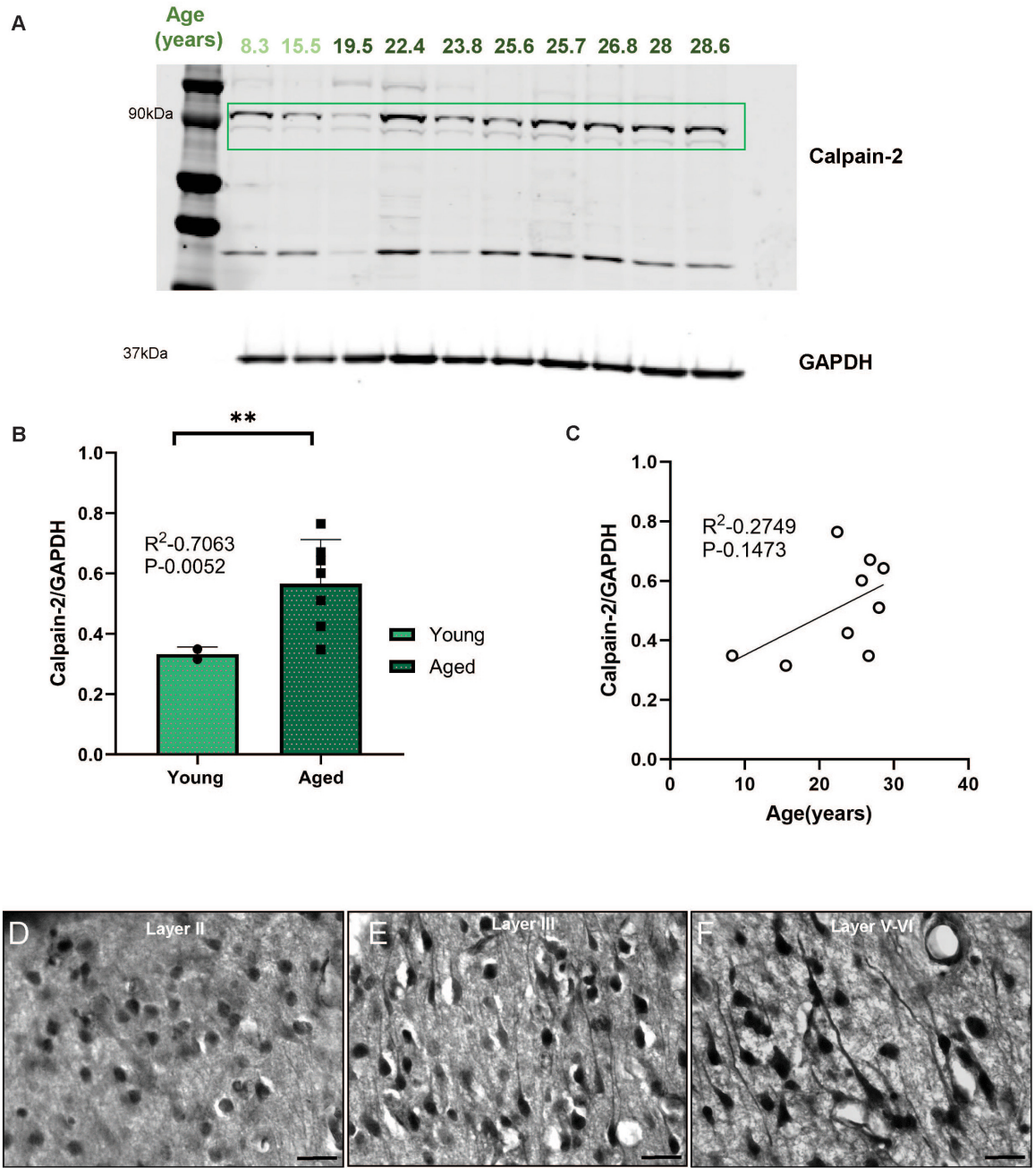

FIGURE 5
(A) Macaque ERC lysate (40 μg) was immunoblotted for calpain-2 (1:1000) and GAPDH (1:10000) across the age span (8.3–28.6 years). Animals are labeled by their age in years and color coded: young animals in light green and aged animals in dark green. **(B)** Expression of calpain-2 normalized by GAPDH is plotted between young (8.3–15.5 years) and aged (22.4–28.6 years). Young animals are denoted by circles and aged animals are denoted by squares. Means between the two groups were compared using a two-tailed unpaired *t*-test (*P = 0.0052). **(C)** The correlation between levels of normalized calpain-2 and age across all animals is fit by a linear regression (R^2 = 0.2749, P = 0.1473). **(D–F)** Immunohistochemistry revealed robust immunolabeling for calpain-2 in aged macaque ERC, particularly in layer II, layer III and layer V–VI, within excitatory neurons along apical and basilar dendrites and in the cell body. Scale bar, 25 μm. **indicates P = 0.001 to 0.01 (highly significant).

Increased pTau with age in ERC

Assays of the aging macaque ERC documented elevated phosphorylated tau, consistent with this region being the earliest site of cortical tau pathology. Previous data had shown evidence of increasing hyperphosphorylation of tau with age in the ERC with both increasing molecular weights and increasing insolubility (Paspalas et al., 2018). The current study builds on this by documenting the rise in pT181, pS214, and pT217. These are all early tau phosphorylation sites (Wesseling et al., 2020), with pT217-tau and pT181-tau emerging as important fluid biomarkers of AD (Barthelemy et al., 2023; Horie et al., 2023; Janelidze et al., 2021).

Plasma pT217-tau in particular is revolutionizing the field, as it heralds future disease, and consistently discriminates AD

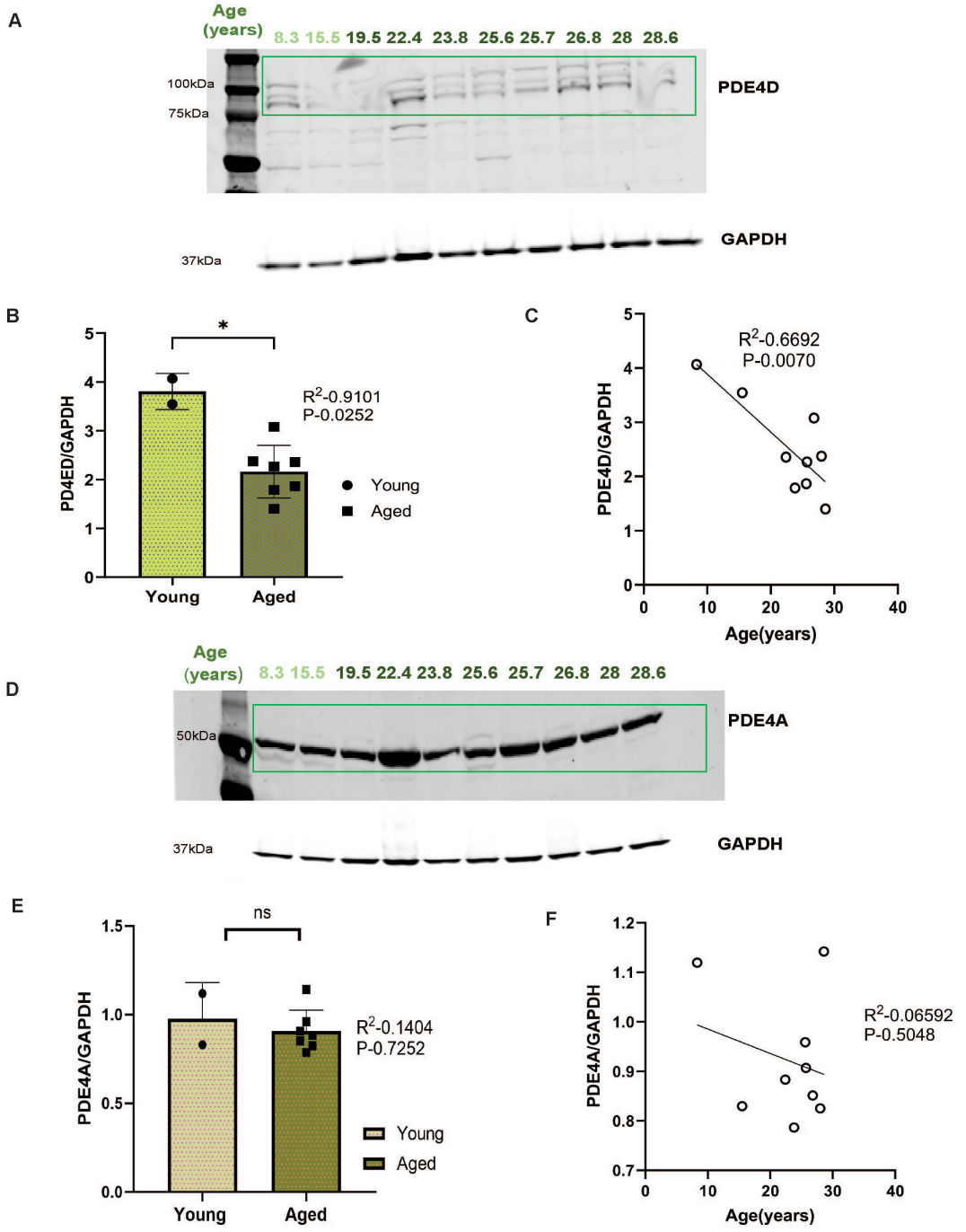

FIGURE 6
(A,D) Macaque ERC lysate (40 μg) was immunoblotted for PDE4D (1:1000), PDE4A (1:1000) and GAPDH (1:10000) across the age span (8.3–28.6 years). Animals are labeled by their age in years and color coded: young animals in in light green and aged animals in dark green. **(B,E)** Expression of PDE4D or PDE4A normalized by GAPDH is plotted between young (8.3–15.5 years) and aged (22.4–28.6 years). Young animals are denoted by circles and aged animals are denoted by squares. Means between the two groups were compared using a two-tailed unpaired *t*-test (*P = 0.0252, P = 0.7252), respectively. **(C,F)** The correlation between levels of normalized PDE4D or PDE4A and age across all animals is fit by a linear regression (R^2 = 0.6692, *P = 0.0070 and R^2 = 0.0659, P = 0.5048), respectively.

from other neurodegenerative diseases, appears in the earliest presymptomatic stages of AD, and correlates strongly with premortem neuropathological tau burden (Barthelemy et al., 2020; Hansson et al., 2023; Janelidze et al., 2020; Mattsson-Carlgren et al., 2023; Olsson et al., 2016; Salvado et al., 2023). Recent data show that the rise in plasma pT217-tau correlates especially well with the appearance of Aβ PET signals in brain (Ashton et al., 2024; Barthelemy et al., 2023; Barthelemy et al., 2024; Janelidze et al., 2024; Janelidze et al., 2021), but little has been known about its rise in brain. Our recent immunoEM studies have documented aggregations of pT217-tau in the dendrites and dendritic spines of layer II ERC neurons from "early" aged (18–19 years) macaques

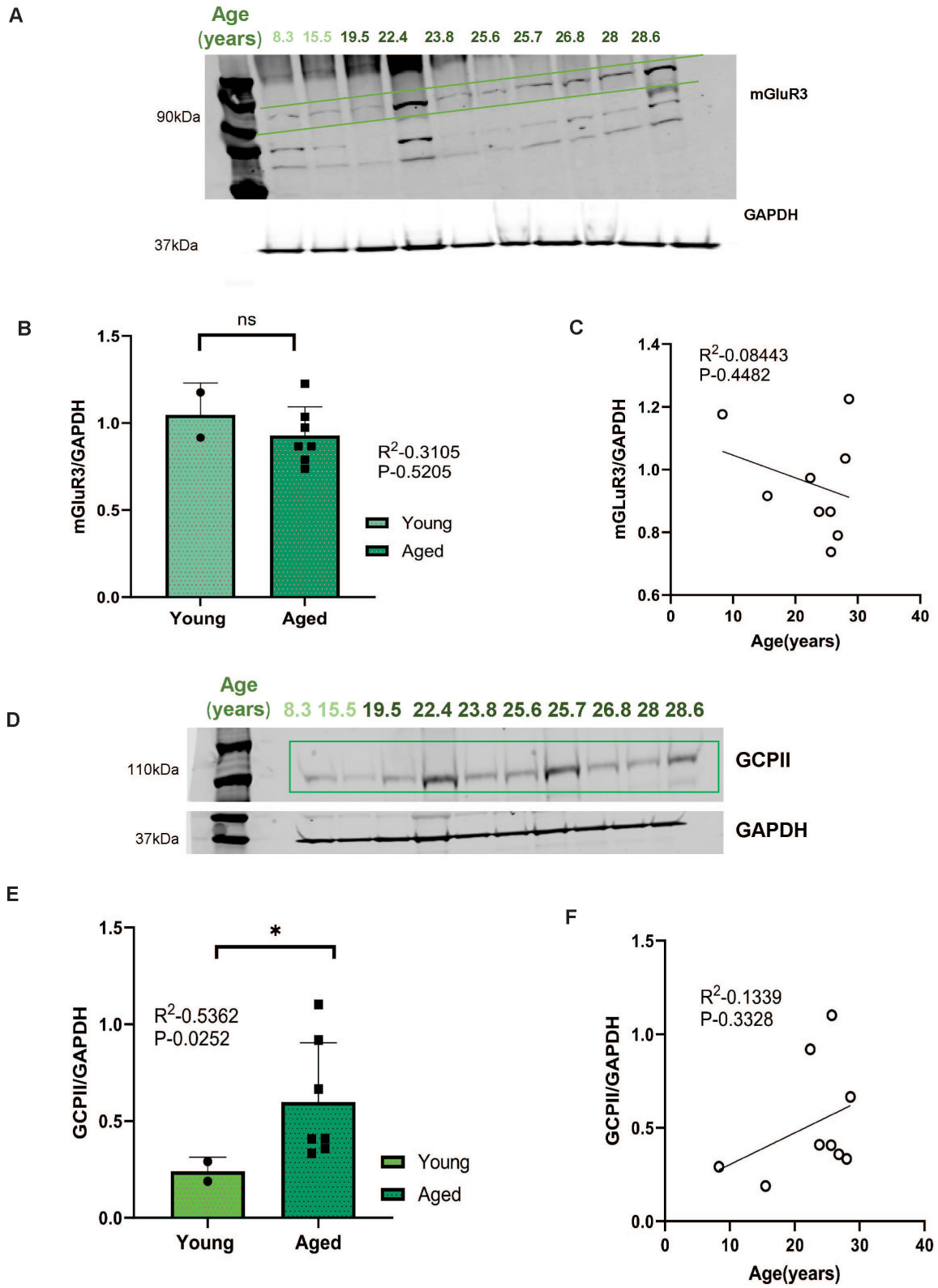

FIGURE 7
(A,D) Macaque ERC lysate (40 μg) was immunoblotted for mGluR3 (1:1000), GCPII (1:1000), and GAPDH (1:10000) across the age span (8.3–28.6 years). Animals are labeled by their age in years and color coded, young animals in in light green and aged animals in dark green. **(B,E)** Expression of mGluR3 or GCPII normalized by GAPDH is plotted between young (8.3–15.5 years) and aged (22.4–28.6 years) age, respectively. Young animals are denoted by circle and aged animals are denoted by square. Means between the two groups were compared using a two-tailed unpaired *t*-test ($P = 0.5205$ and $^*P = 0.0252$). **(C,F)** The correlation between levels of normalized mGluR3, GCPII and age across all animals is fit by a linear regression ($R^2 = 0.0844$, $P = 0.4482$, and $R^2 = 0.1339$, $P = 0.328$), respectively.

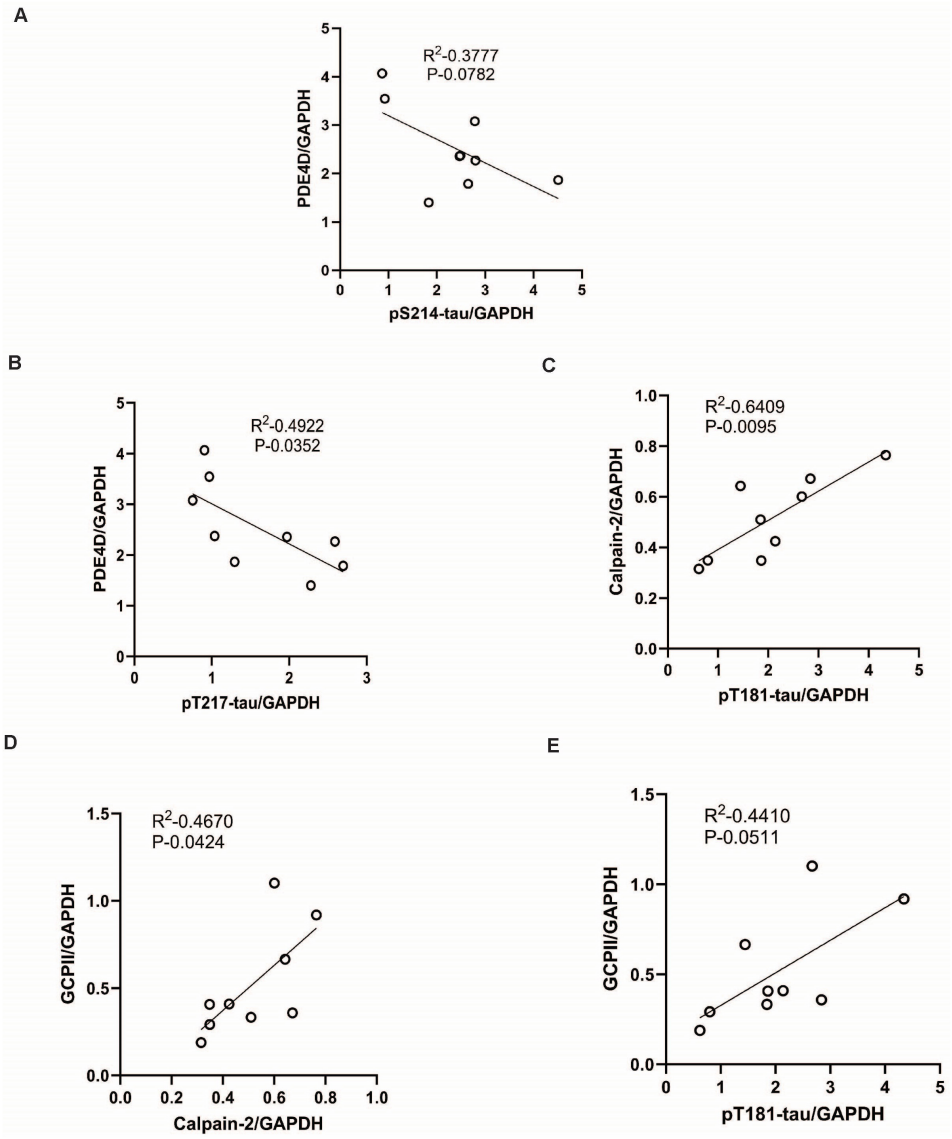

FIGURE 8
(A) Correlation between levels of pS214-tau by GAPDH (x axis) and PDE4D by GAPDH (y axis) is fit by a linear regression (R^2 = 0.3777, P = 0.0782). Animals aged (22.4 and 28 years) exhibit similar expression levels, and the graph shows overlap between these two data points. **(B)** Correlation between levels of pT217-tau by GAPDH (x axis) and PDE4D by GAPDH (y axis) is fit by a linear regression (R^2 = 0.4922, *P = 0.0352). **(C)** Correlation between levels of pT181-tau by GAPDH (x axis) and calpain-2 by GAPDH (y axis) is fit by a linear regression (R^2 = 0.6409, *P = 0.0095). **(D)** Correlation between levels of calpain-2 by GAPDH (x axis) and GCPII by GAPDH (y axis) is fit by a linear regression (R^2 = 0.4670, *P = 0.0424). **(E)** Correlation between levels of pT181-tau by GAPDH (x axis) and GCPII by GAPDH (y axis) is fit by a linear regression (R^2 = 0.4410, P = 0.0511).

(Datta et al., 2024). Nanoscale imaging also demonstrated pT217-tau trafficking between synapses, where it can be captured in extracellular fluid (Datta et al., 2024), helping to explain how this pTau species reaches CSF and plasma as a fluid biomarker.

Support for dysregulated cAMP-calcium inflammatory signaling with age

Decades of research indicate that calcium dysregulation is an early driver of AD pathology in both sporadic and autosomal dominant disease (Alzheimer's Association Calcium Hypothesis, 2017; Gant et al., 2018; Khachaturian, 1994), with elevated calcium in the cytosol, rather than stored in the SER, activating calpain-2 to disinhibit GSK3β and cdk5 to hyperphosphorylate tau (Arnsten et al., 2021b; Arnsten et al., 2021c). cAMP-PKA calcium signaling plays an important role in driving calcium release out of the SER, which is regulated by PDE4D anchored to the SER to reduce cAMP-PKA signaling (Bathla et al., 2023). The current study showed a loss of PDE4D in the aged ERC, suggesting disrupted regulation of cAMP-PKA signaling. The current study replicated earlier data showing that pRyR2 expression is already evident in the ERC in middle age, but this did not increase with age. We did find increased expression of calpain-2, which plays an important role in driving both tau hyperphosphorylation and autophagic degeneration, and is associated with neurofibrillary tangles in AD brains (Adamec

et al., 2002; Grynspan et al., 1997). Decreased PDE4D levels and increased calpain-2 levels correlated with increased pTau levels in the aged macaque ERC, consistent with dysregulated cAMP-calcium signaling contributing to tau hyperphosphorylation.

mGluR3 intact as potential therapeutic target: focus on the role of GCPII inhibitors

While mGluR3 have traditionally been considered presynaptic receptors based on their localization in rodent (Woo et al., 2022), new data show that mGluR3 have a very different and important role in primate higher cortical circuits, where they are post-synaptic and regulate cAMP-calcium signaling (Arnsten and Wang, 2020). This has been seen in both dlPFC (Jin et al., 2018a) and more recently in the macaque ERC (Datta et al., 2023). mGluR3 are stimulated not only by glutamate, but by NAAG which is selective for mGluR3 (Neale and Olszewski, 2019). However, NAAG-mGluR3 signaling is a target of inflammation when GCPII catabolizes NAAG (Arteaga Cabeza et al., 2021; Zhang et al., 2016). The current study found an age-related increase in GCPII in the macaque ERC which correlated with increased pTau expression. These data are consistent with previous work showing that chronic GCPII inhibition in aged monkeys reduces pT217-tau levels in the ERC and dlPFC, as well as in blood (Bathla et al., 2023). This previous study also found a strong correlation between levels of GCPII activity and pT217-tau expression in dlPFC (Bathla et al., 2023), emphasizing the potential relevance of this pathway to early-stage AD pathology. As the current study found that mGluR3 expression remains relatively intact, this beneficial substrate appears to remain in dlPFC, further encouraging the development of GCPII inhibitors for human trials.

Conclusion

Our findings reveal an advancing age-related decrease in PDE4 that is associated with calcium dysregulation and which may lead to early-stage tau hyperphosphorylation in ERC. The identification of notable alterations in proteins associated with tau pathology and calcium signaling should help in the development of more targeted and effective interventions to slow AD progression.

Data availability statement

The original contributions presented in this study are included in this article/supplementary material, further inquiries can be directed to the corresponding authors.

Ethics statement

The animal study was approved by American Association for Accreditation of Laboratory Animal Care (AAALAC). The study was conducted in accordance with the local legislation and institutional requirements.

Author contributions

SB: Conceptualization, Formal Analysis, Investigation, Methodology, Validation, Writing – original draft, Writing – review and editing. DD: Conceptualization, Formal Analysis, Investigation, Methodology, Validation, Writing – original draft, Writing – review and editing. DB: Methodology, Writing – review and editing. EW: Methodology, Writing – review and editing. AD: Methodology, Writing – review and editing. JA: Methodology, Writing – review and editing. AA: Conceptualization, Funding acquisition, Resources, Supervision, Writing – review and editing. AN: Conceptualization, Funding acquisition, Resources, Supervision, Writing – review and editing.

Funding

The author(s) declare that financial support was received for the research and/or publication of this article. This work was primarily supported by National Institute of Health (NIH) R21 grant AG079145-01, KL2 TR001862, Alzheimer's Association Research Grant AARGD-23-1150568 to DD and RO1 grant AG061190-01 to AA. This work was also partly supported by the American Federation for Aging Research (AFAR) Faculty Transition Award and support from Yale Alzheimer's Disease Research Center (ADRC) P30AG066508 to AN, and a Developmental Project Award to DD.

Acknowledgments

We thank Caroline Zeiss, Dan Holden, Lisa Ciavarella, Tracy Sadlon, Sam Johnson, and Michelle Wilson for their technical expertise and assistance with animals.

Conflict of interest

The authors declare that the research was conducted in the absence of any commercial or financial relationships that could be construed as a potential conflict of interest.

Generative AI statement

The authors declare that no Generative AI was used in the creation of this manuscript.

Publisher's note

References

Adamec, E., Mohan, P., Vonsattel, J., and Nixon, R. (2002). Calpain activation in neurodegenerative diseases: Confocal immunofluorescence study with antibodies specifically recognizing the active form of calpain 2. *Acta Neuropathol.* 104, 92–104. doi: 10.1007/s00401-002-0528-6

Ahmed, Z., Cooper, J., Murray, T., Garn, K., McNaughton, E., Clarke, H., et al. (2014). A novel in vivo model of tau propagation with rapid and progressive neurofibrillary tangle pathology: The pattern of spread is determined by connectivity, not proximity. *Acta Neuropathol.* 127, 667–683. doi: 10.1007/s00401-014-1254-6

Alzheimer's Association Calcium Hypothesis (2017). Calcium Hypothesis of Alzheimer's disease and brain aging: A framework for integrating new evidence into a comprehensive theory of pathogenesis. *Alzheimers Dement.* 13, 178–182 e117. doi: 10.1016/j.jalz.2016.12.006.

Arnsten, A., and Wang, M. (2020). The evolutionary expansion of mGluR3-NAAG-GCPII signaling: Relevance to human intelligence and cognitive disorders. *Am. J. Psychiatry* 177, 1103–1106. doi: 10.1176/appi.ajp.2020.20101458

Arnsten, A., Datta, D., and Preuss, T. (2021b). Studies of aging nonhuman primates illuminate the etiology of early-stage Alzheimer's-like neuropathology: An evolutionary perspective. *Am. J. Primatol.* 83:e23254. doi: 10.1002/ajp.23254

Arnsten, A., Datta, D., and Wang, M. (2021c). The genie in the bottle-magnified calcium signaling in dorsolateral prefrontal cortex. *Mol. Psychiatry* 26, 3684–3700. doi: 10.1038/s41380-020-00973-3

Arnsten, A., Datta, D., Del Tredici, K., and Braak, H. (2020). Hypothesis: Tau pathology is an initiating factor in sporadic Alzheimer's disease. *Alzheimers Dement.* 17, 115–124. doi: 10.1002/alz.12192

Arnsten, A., Datta, D., Del Tredici, K., and Braak, H. (2021a). Hypothesis: Tau pathology is an initiating factor in sporadic Alzheimer's disease. *Alzheimers Dement.* 17, 115–124. doi: 10.1002/alz.12192

Arnsten, A., Datta, D., Leslie, S., Yang, S., Wang, M., and Nairn, A. (2019). Alzheimer's-like pathology in aging rhesus macaques: Unique opportunity to study the etiology and treatment of Alzheimer's disease. *Proc. Natl. Acad. Sci. U S A.* 116, 26230–26238. doi: 10.1073/pnas.1903671116

Arteaga Cabeza, O., Zhang, Z., Smith Khoury, E., Sheldon, R., Sharma, A., Zhang, F., et al. (2021). Neuroprotective effects of a dendrimer-based glutamate carboxypeptidase inhibitor on superoxide dismutase transgenic mice after neonatal hypoxic-ischemic brain injury. *Neurobiol. Dis.* 148:105201. doi: 10.1016/j.nbd.2020.105201

Ashton, N., Brum, W., Di Molfetta, G., Benedet, A., Arslan, B., Jonaitis, E., et al. (2024). Diagnostic accuracy of a plasma phosphorylated Tau 217 immunoassay for Alzheimer disease pathology. *JAMA Neurol.* 81, 255–263. doi: 10.1001/jamaneurol.2023.5319

Barthelemy, N., Bateman, R., Hirtz, C., Marin, P., Becher, F., Sato, C., et al. (2020). Cerebrospinal fluid phospho-tau T217 outperforms T181 as a biomarker for the differential diagnosis of Alzheimer's disease and PET amyloid-positive patient identification. *Alzheimers Res. Ther.* 12:26. doi: 10.1186/s13195-020-00596-4

Barthelemy, N., Saef, B., Li, Y., Gordon, B., He, Y., Horie, K., et al. (2023). CSF tau phosphorylation occupancies at T217 and T205 represent improved biomarkers of amyloid and tau pathology in Alzheimer's disease. *Nat. Aging* 3, 391–401. doi: 10.1038/s43587-023-00380-7

Barthelemy, N., Salvadó, G., Schindler, S., He, Y., Janelidze, S., Collij, L., et al. (2024). Highly accurate blood test for Alzheimer's disease is similar or superior to clinical cerebrospinal fluid tests. *Nat. Med.* 30, 1085–1095. doi: 10.1038/s41591-024-02869-z

Bartus, R., Fleming, D., and Johnson, H. (1978). Aging in the rhesus monkey: Debilitating effects on short-term memory. *J. Gerontol.* 33, 858–871. doi: 10.1093/geronj/33.6.858

Bathla, S., Datta, D., Liang, F., Barthelemy, N., Wiseman, R., Slusher, B., et al. (2023). Chronic GCPII (glutamate-carboxypeptidase-II) inhibition reduces pT217Tau levels in the entorhinal and dorsolateral prefrontal cortices of aged macaques. *Alzheimers Dement.* 9:e12431. doi: 10.1002/trc2.12431

Baudry, M., Chou, M., and Bi, X. (2013). Targeting calpain in synaptic plasticity. *Expert. Opin. Ther. Targets* 17, 579–592. doi: 10.1517/14728222.2013.766169

Bedada, F., Martindale, J., Arden, E., and Metzger, J. (2016). Molecular inotropy mediated by cardiac miR-based PDE4D/PRKAR1α/phosphoprotein signaling. *Sci. Rep.* 6:36803. doi: 10.1038/srep36803

Braak, H., and Braak, E. (1991). Neuropathological stageing of Alzheimer-related changes. *Acta Neuropathol.* 82, 239–259. doi: 10.1007/BF00308809

Braak, H., and Braak, E. (1992). The human entorhinal cortex: Normal morphology and lamina-specific pathology in various diseases. *Neurosci. Res.* 15, 6–31. doi: 10.1016/0168-0102(92)90014-4

Braak, H., and Del Tredici, K. (2015). Neuroanatomy and pathology of sporadic Alzheimer's disease. *Adv. Anat. Embryol. Cell. Biol.* 215, 1–162.

Braak, H., and Del Tredici, K. (2015). The preclinical phase of the pathological process underlying sporadic Alzheimer's disease. *Brain* 138, 2814–2833. doi: 10.1093/brain/awv236

Calafate, S., Buist, A., Miskiewicz, K., Vijayan, V., Daneels, G., de Strooper, B., et al. (2015). Synaptic contacts enhance cell-to-cell Tau pathology propagation. *Cell Rep.* 11, 1176–1183. doi: 10.1016/j.celrep.2015.04.043

Carlyle, B., Nairn, A., Wang, M., Yang, Y., Jin, L., Simen, A., et al. (2014). cAMP-PKA phosphorylation of tau confers risk for degeneration in aging association cortex. *Proc. Natl. Acad. Sci. U S A.* 111, 5036–5041. doi: 10.1073/pnas.1322360111

Colin, M., Dujardin, S., Schraen-Maschke, S., Meno-Tetang, G., Duyckaerts, C., Courade, J., et al. (2020). From the prion-like propagation hypothesis to therapeutic strategies of anti-tau immunotherapy. *Acta Neuropathol.* 139, 3–25. doi: 10.1007/s00401-019-02087-9

Datta, D., Enwright, J., Arion, D., Paspalas, C., Morozov, Y., Lewis, D., et al. (2020). Mapping phosphodiesterase 4D (PDE4D) in macaque dorsolateral prefrontal cortex: Postsynaptic compartmentalization in layer III pyramidal cell circuits. *Front. Neuroanat.* 14:578483. doi: 10.3389/fnana.2020.578483

Datta, D., Leslie, S., Wang, M., Morozov, Y., Yang, S., Mentone, S., et al. (2021). Age-related calcium dysregulation linked with tau pathology and impaired cognition in non-human primates. *Alzheimers Dement.* 17, 920–932. doi: 10.1002/alz.12325

Datta, D., Perone, I., Morozov, Y., Arellano, J., Duque, A., Rakic, P., et al. (2023). Localization of PDE4D, HCN1 channels, and mGluR3 in rhesus macaque entorhinal cortex may confer vulnerability in Alzheimer's disease. *Cereb. Cortex* 33, 11501–11516. doi: 10.1093/cercor/bhad382

Datta, D., Perone, I., Wijegunawardana, D., Liang, F., Morozov, Y., Arellano, J., et al. (2024). Nanoscale imaging of pT217-tau in aged rhesus macaque entorhinal and dorsolateral prefrontal cortex: Evidence of interneuronal trafficking and early-stage neurodegeneration. *Alzheimers Dement.* 20, 2843–2860. doi: 10.1002/alz.13737

de Calignon, A., Polydoro, M., Suárez-Calvet, M., William, C., Adamowicz, D., Kopeikina, K., et al. (2012). Propagation of tau pathology in a model of early Alzheimer's disease. *Neuron* 73, 685–697. doi: 10.1016/j.neuron.2011.11.033

Dujardin, S., Bégard, S., Caillierez, R., Lachaud, C., Carrier, S., Lieger, S., et al. (2018). Different tau species lead to heterogeneous tau pathology propagation and misfolding. *Acta Neuropathol. Commun.* 6:132. doi: 10.1186/s40478-018-0637-7

Fu, H., Hardy, J., and Duff, K. (2018). Selective vulnerability in neurodegenerative diseases. *Nat. Neurosci.* 21, 1350–1358. doi: 10.1038/s41593-018-0221-2

Gant, J., Kadish, I., Chen, K., Thibault, O., Blalock, E., Porter, N., et al. (2018). Aging-related calcium dysregulation in rat entorhinal neurons homologous with the human entorhinal neurons in which Alzheimer's disease neurofibrillary tangles first appear. *J. Alzheimers Dis.* 66, 1371–1378. doi: 10.3233/JAD-180618

Gibson, G., and Peterson, C. (1987). Calcium and the aging nervous system. *Neurobiol. Aging* 8, 329–343. doi: 10.1016/0197-4580(87)90072-8

Goñi-Oliver, P., Lucas, J., Avila, J., and Hernández, F. (2007). N-terminal cleavage of GSK-3 by calpain: A new form of GSK-3 regulation. *J. Biol. Chem.* 282, 22406–22413. doi: 10.1074/jbc.M702793200

Grynspan, F., Griffin, W., Cataldo, A., Katayama, S., and Nixon, R. (1997). Active site-directed antibodies identify calpain II as an early-appearing and pervasive component of neurofibrillary pathology in Alzheimer's disease. *Brain Res.* 763, 145–158. doi: 10.1016/s0006-8993(97)00384-3

Hansson, O., Blennow, K., Zetterberg, H., and Dage, J. (2023). Blood biomarkers for Alzheimer's disease in clinical practice and trials. *Nat. Aging* 3, 506–519. doi: 10.1038/s43587-023-00403-3

Herndon, J., Moss, M., Rosene, D., and Killiany, R. (1997). Patterns of cognitive decline in aged rhesus monkeys. *Behav. Brain Res.* 87, 25–34. doi: 10.1016/s0166-4328(96)02256-5

Higuchi, M., Iwata, N., Matsuba, Y., Takano, J., Suemoto, T., Maeda, J., et al. (2012). Mechanistic involvement of the calpain-calpastatin system in Alzheimer neuropathology. *FASEB J.* 26, 1204–1217. doi: 10.1096/fj.11-187740

Horie, K., Salvadó, G., Barthélemy, N., Janelidze, S., Li, Y., He, Y., et al. (2023). CSF MTBR-tau243 is a specific biomarker of tau tangle pathology in Alzheimer's disease. *Nat. Med.* 29, 1954–1963. doi: 10.1038/s41591-023-02443-z

Hyman, B., Van Hoesen, G., Kromer, L., and Damasio, A. (1986). Perforant pathway changes and the memory impairment of Alzheimer's disease. *Ann. Neurol.* 20, 472–481. doi: 10.1002/ana.410200406

Imamura, K., Sahara, N., Kanaan, N., Tsukita, K., Kondo, T., Kutoku, Y., et al. (2016). Calcium dysregulation contributes to neurodegeneration in FTLD patient iPSC-derived neurons. *Sci. Rep.* 6:34904. doi: 10.1038/srep34904

Insel, N., Ruiz-Luna, M., Permenter, M., Vogt, J., Erickson, C., and Barnes, C. (2008). Aging in rhesus macaques is associated with changes in novelty preference and altered saccade dynamics. *Behav. Neurosci.* 122, 1328–1342. doi: 10.1037/a0012928

Janelidze, S., Barthélemy, N., Salvadó, G., Schindler, S., Palmqvist, S., Mattsson-Carlgren, N., et al. (2024). Plasma phosphorylated Tau 217 and Aβ42/40 to predict early brain Aβ accumulation in people without cognitive impairment. *JAMA Neurol.* 81, 947–957. doi: 10.1001/jamaneurol.2024.2619

Janelidze, S., Berron, D., Smith, R., Strandberg, O., Proctor, N., Dage, J., et al. (2021). Associations of plasma phospho-Tau217 levels with tau positron emission tomography in early Alzheimer disease. *JAMA Neurol.* 78, 149–156. doi: 10.1001/jamaneurol.2020.4201

Janelidze, S., Stomrud, E., Smith, R., Palmqvist, S., Mattsson, N., Airey, D., et al. (2020). Cerebrospinal fluid p-tau217 performs better than p-tau181 as a biomarker of Alzheimer's disease. *Nat. Commun.* 11:1683. doi: 10.1038/s41467-020-15436-0

Jin, L., Wang, M., Galvin, V., Lightbourne, T., Conn, P., Arnsten, A., et al. (2018a). mGluR2 versus mGluR3 metabotropic glutamate receptors in primate dorsolateral prefrontal cortex: Postsynaptic mGluR3 strengthen working memory networks. *Cereb. Cortex* 28, 974–987. doi: 10.1093/cercor/bhx005

Jin L.E., Wang M., Galvin V.C., Lightbourne T.C., Conn P.J., Arnsten A.F.T., et al. (2018b). mGluR2 vs. mGluR3 in Primate Prefrontal Cortex: Postsynaptic mGluR3 Strengthen Cognitive Networks. *Cereb. Cortex*. 28, 974–987.

Kaar, A., Weir, M., and Rae, M. (2024). Altered neuronal group 1 metabotropic glutamate receptor- and endoplasmic reticulum-mediated Ca2+ signaling in two rodent models of Alzheimer's disease. *Neurosci. Lett.* 823:137664. doi: 10.1016/j.neulet.2024.137664

Katzeff, J., Bright, F., Lo, K., Kril, J., Connolly, A., Crossett, B., et al. (2020). Altered serum protein levels in frontotemporal dementia and amyotrophic lateral sclerosis indicate calcium and immunity dysregulation. *Sci. Rep.* 10:13741. doi: 10.1038/s41598-020-70687-7

Kaufman, S., Del Tredici, K., Thomas, T., Braak, H., and Diamond, M. (2018). Tau seeding activity begins in the transentorhinal/entorhinal regions and anticipates phospho-tau pathology in Alzheimer's disease and PART. *Acta Neuropathol.* 136, 57–67. doi: 10.1007/s00401-018-1855-6

Khachaturian, Z. (1994). Calcium hypothesis of Alzheimer's disease and brain aging. *Ann. N. Y. Acad. Sci.* 747, 1–11. doi: 10.1111/j.1749-6632.1994.tb44398.x

Lacampagne, A., Liu, X., Reiken, S., Bussiere, R., Meli, A., Lauritzen, I., et al. (2017). Post-translational remodeling of ryanodine receptor induces calcium leak leading to Alzheimer's disease-like pathologies and cognitive deficits. *Acta Neuropathol.* 134, 749–767. doi: 10.1007/s00401-017-1733-7

Leslie, S., Kanyo, J., Datta, D., Wilson, R., Zeiss, C., Duque, A., et al. (2021). Simple, single-shot phosphoproteomic Analysis of heat-stable tau identifies age-related changes in pS235- and pS396-Tau levels in non-human primates. *Front. Aging Neurosci.* 13:767322. doi: 10.3389/fnagi.2021.767322

Lewis, D., Campbell, M., Terry, R., and Morrison, J. (1987). Laminar and regional distributions of neurofibrillary tangles and neuritic plaques in Alzheimer's disease: A quantitative study of visual and auditory cortices. *J. Neurosci.* 7, 1799–1808. doi: 10.1523/JNEUROSCI.07-06-01799.1987

Liu, J., and Li, L. (2019). Targeting autophagy for the treatment of Alzheimer's disease: Challenges and opportunities. *Front. Mol. Neurosci.* 12:203. doi: 10.3389/fnmol.2019.00203

Matsuo, E., Shin, R., Billingsley, M., Van deVoorde, A., O'Connor, M., Trojanowski, J., et al. (1994). Biopsy-derived adult human brain tau is phosphorylated at many of the same sites as Alzheimer's disease paired helical filament tau. *Neuron* 13, 989–1002. doi: 10.1016/0896-6273(94)90264-x

Mattsson-Carlgren, N., Salvadó, G., Ashton, N., Tideman, P., Stomrud, E., Zetterberg, H., et al. (2023). Prediction of longitudinal cognitive decline in preclinical Alzheimer disease using plasma biomarkers. *JAMA Neurol.* 80, 360–369. doi: 10.1001/jamaneurol.2022.5272

Neale, J., and Olszewski, R. (2019). A role for N-acetylaspartylglutamate (NAAG) and mGluR3 in cognition. *Neurobiol. Learn. Mem.* 158, 9–13. doi: 10.1016/j.nlm.2019.01.006

Olsson, B., Lautner, R., Andreasson, U., Öhrfelt, A., Portelius, E., Bjerke, M., et al. (2016). CSF and blood biomarkers for the diagnosis of Alzheimer's disease: A systematic review and meta-analysis. *Lancet Neurol.* 15, 673–684. doi: 10.1016/S1474-4422(16)00070-3

Paspalas, C., Carlyle, B., Leslie, S., Preuss, T., Crimins, J., Huttner, A., et al. (2018). The aged rhesus macaque manifests Braak stage III/IV Alzheimer's-like pathology. *Alzheimers Dement.* 14, 680–691. doi: 10.1016/j.jalz.2017.11.005

Paspalas, C., Wang, M., and Arnsten, A. (2013). Constellation of HCN channels and cAMP regulating proteins in dendritic spines of the primate prefrontal cortex: Potential substrate for working memory deficits in schizophrenia. *Cereb. Cortex* 23, 1643–1654. doi: 10.1093/cercor/bhs152

Ramos, B., Birnbaum, S., Lindenmayer, I., Newton, S., Duman, R., and Arnsten, A. (2003). Dysregulation of protein kinase a signaling in the aged prefrontal cortex: New strategy for treating age-related cognitive decline. *Neuron* 40, 835–845. doi: 10.1016/s0896-6273(03)00694-9

Salvado, G., Ossenkoppele, R., Ashton, N., Beach, T., Serrano, G., Reiman, E., et al. (2023). Specific associations between plasma biomarkers and postmortem amyloid plaque and tau tangle loads. *EMBO Mol. Med.* 15:e17123. doi: 10.15252/emmm.202217123

Wang, Y., Zhang, Y., Hu, W., Xie, S., Gong, C., Iqbal, K., et al. (2015). Rapid alteration of protein phosphorylation during postmortem: Implication in the study of protein phosphorylation. *Sci. Rep.* 5:15709. doi: 10.1038/srep15709

Webber, E., Fivaz, M., Stutzmann, G., and Griffioen, G. (2023). Cytosolic calcium: Judge, jury and executioner of neurodegeneration in Alzheimer's disease and beyond. *Alzheimers Dement.* 19, 3701–3717. doi: 10.1002/alz.13065

Wesseling, H., Mair, W., Kumar, M., Schlaffner, C., Tang, S., Beerepoot, P., et al. (2020). Tau PTM profiles identify patient heterogeneity and stages of Alzheimer's disease. *Cell* 183, 1699–1713.e13. doi: 10.1016/j.cell.2020.10.029.

Whitney, K., Song, W., Sharma, A., Dangoor, D., Farrell, K., Krassner, M., et al. (2024). Single-cell transcriptomic and neuropathologic analysis reveals dysregulation of the integrated stress response in progressive supranuclear palsy. *Acta Neuropathol.* 148, 1–22. doi: 10.1007/s00401-024-02823-w

Wilson, D., Cookson, M., Van Den Bosch, L., Zetterberg, H., Holtzman, D., and Dewachter, I. (2023). Hallmarks of neurodegenerative diseases. *Cell* 186, 693–714. doi: 10.1016/j.cell.2022.12.032

Woo, E., Datta, D., and Arnsten, A. (2022). Glutamate metabotropic receptor type 3 (mGlu3) localization in the rat prelimbic medial prefrontal cortex. *Front. Neuroanat.* 16:849937. doi: 10.3389/fnana.2022.849937

Yang, S., Datta, D., Woo, E., Duque, A., Morozov, Y. M., Arellano, J., et al. (2022). Inhibition of glutamate-carboxypeptidase-II in dorsolateral prefrontal cortex: Potential therapeutic target for neuroinflammatory cognitive disorders. *Mol. Psychiatry* 27, 4252–4263. doi: 10.1038/s41380-022-01656-x

Zhang, S., Crossley, C., and Yuan, Q. (2024). Neuronal vulnerability of the entorhinal cortex to tau pathology in Alzheimer's disease. *Br. J. Biomed. Sci.* 81:13169. doi: 10.3389/bjbs.2024.13169

Zhang, Z., Bassam, B., Thomas, A., Williams, M., Liu, J., Nance, E., et al. (2016). Maternal inflammation leads to impaired glutamate homeostasis and up-regulation of glutamate carboxypeptidase II in activated microglia in the fetal/newborn rabbit brain. *Neurobiol. Dis.* 94, 116–128. doi: 10.1016/j.nbd.2016.06.010